Journal of Environmental Management 256 (2020) 109957

Contents lists available at ScienceDirect

Journal of Environmental Management

journal homepage: http://www.elsevier.com/locate/jenvman

Research article

Bioflocculation and settling studies of native wastewater filamentous cyanobacteria using different cultivation systems for a low-cost and easy to control harvesting process

Floriana Iasimone [a,*], Jordan Seira [b], Elie Desmond-Le Quéméner [b], Antonio Panico [c], Vincenzo De Felice [a], Francesco Pirozzi [d], Jean-Philippe Steyer [b]

[a] Università degli Studi del Molise, Dipartimento di Bioscienze e Territorio, C.da Fonte Lappone, 86090, Pesche (IS), Italy
[b] LBE, Univ Montpellier, INRA, 102 Avenue des Étangs, 11100, Narbonne, France
[c] Università Telematica Pegaso, Piazza Trieste e Trento 48, 80132, Napoli, Italy
[d] Università degli Studi di Napoli, Dipartimento di Ingegneria Civile Edile Ambientale, Via Claudio 21, 80125, Napoli, Italy

ARTICLE INFO

Keywords:
Bioflocculation
Filamentous cyanobacteria
Urban wastewater
Sedimentation model

ABSTRACT

Bioflocculation phenomena for filamentous cyanobacteria were studied and analysed in two different cultivation systems (i.e. based on air-bubbling and on shaking) and for different initial biomass concentrations. Floc formation and biomass settling were monitored during batch cultivation tests according to an innovative protocol. Results showed that the two cultivation systems enhanced two different flocculation behaviours: air bubbling led to the formation of small and dense flocs, while the shaking table resulted in larger (14 mm^2 vs 4 mm^2) but mechanically weaker flocs. Floc analysis evidenced that the different mixing systems also affected the speciation of biomass. A mathematical model was developed to simulate and predict the settling performance during the bioflocculation process of filamentous cyanobacteria. Natural settling was examined at different phases of biomass growth. Optimal conditions were obtained at the end of the exponential growth phase, when 70% of the total cultivated biomass could be recovered.

1. Introduction

According to current worldwide trends, the global consumption of fossil-based fuels is continuously increasing, thus aggravating pollution of the environment, amplifying risks for human health and accelerating climate change, while the planetary reservoirs are diminishing significantly (Pradhan et al., 2017). A common solution for these environmental deterioration and energy depletion issues could be found in the development of bioenergy based on biomass conversion. Among all biomass sources, microalgae and cyanobacteria are currently the object of considerable renewed attention as feedstock for large-scale bioenergy production (Singh et al., 2016). They present a higher photosynthetic efficiency and biomass productivity compared to terrestrial crops and are capable of growing in both clean water as well as wastewater. Thus they do not require the use of arable land nor compete with food crop cultivation (Gouveia et al., 2016). Indeed, wastewater treatment microalgae and cyanobacteria ponds are noteworthy because they represent an economically feasible method of appropriate biomass production for conversion into biofuels. The resulting environmental impact can therefore be negligible while it can also be a particularly economical solution (Lardon et al., 2009; Park et al., 2015). Despite recent intensive efforts for rendering microalgae and cyanobacteria-based biofuel economically viable when compared to fossil fuels, a number of obstacles still impede the full success of this methodology. One of these main obstacles for large scale application is biomass harvesting, accounting for 20–30% of the total costs of microalgae and cyanobacteria biomass cultivation (Christenson and Sims, 2011). At present, the most common systems used for biomass harvesting involve centrifugation and chemical flocculation although these cannot be applied at large scales due to high costs and undesirable by-products, respectively (Barros et al., 2015): indeed, centrifugation is a high-energy consuming process while chemical flocculation entails secondary pollution in the liquid effluent. A valid alternative could be the natural flocculation of the biomass. This process, scientifically known as bioflocculation, represents an attractive solution for biomass harvesting since it is inexpensive, has a low energy demand, is non-toxic

* Corresponding author.
E-mail address: floriana.iasimone@unimol.it (F. Iasimone).

https://doi.org/10.1016/j.jenvman.2019.109957
Received 27 April 2019; Received in revised form 7 November 2019; Accepted 3 December 2019

and does not require the use of flocculants, thus enabling the reuse of a harmless cultivation medium (Alam et al., 2016; Salim et al., 2011). Bioflocculation refers to naturally induced flocculation due to biopolymers secreted by live microalgae cells as well as bacteria (Ndikubwimana et al., 2015). Recent studies have investigated the bioflocculation process occurring for microalgal-bacterial, microalgal-fungal or microalgal-microalgal interactions (Alam et al., 2016). However, cyanobacteria flocculation remains poorly explored. In cases of wastewater treated with microalgal and cyanobacterial cultures, high flocculation efficiencies have been observed when filamentous cyanobacteria dominate the microalgae-cyanobacteria consortium (Su et al., 2011). Bench scale studies have demonstrated that gliding and colliding of cyanobacteria filaments produce reticulates and regular, well-shaped structures (Shepard and Sumner, 2010). These findings suggest cyanobacteria could promote natural flocculation if cultivated alone or in combination with microalgae, other bacteria or fungi.

Based on these initial observations, the present work focusses on the bioflocculation of a wastewater native filamentous cyanobacteria consortium in order to assess its potential application to large scale wastewater treatment systems. Shepard and Sumner (Su et al., 2011) observed that the geometry of cyanobacteria structures, their morphology and the time required for macroscopic floc formation depend on cell density. Furthermore, studies on cell aggregation (Castenholz, 1967; Koblížek and Komenda, 2000) demonstrated how turbulence generated by physical mixing systems also affects the aggregation capacity. The present study was thus conducted on a synthetic growth medium in order to achieve reproducible operating conditions. Two different mixing conditions and various initial cyanobacteria concentrations were investigated. A sedimentation mathematical model was then developed to simulate the settling dynamics and to assess the main influencing factors.

2. Materials and methods

2.1. Inoculum cultivation

A naturally grown biofilm was collected from the secondary clarifier of a municipal wastewater plant (41.6082N, 14.273E) from Isernia (Molise, Italy) and was cultivated in a modified Bold Basal Medium (BBM) to provide controlled and reproducible conditions. The medium contained the following elements: 250 mg.L^{-1} $NaNO_3$, 25 mg.L^{-1} $CaCl_2 \cdot 2H_2O$, 75 mg.L^{-1} $MgSO_4 \cdot 7H_2O$, 75 mg.L^{-1} K_2HPO_4, 175 mg.L^{-1} KH_2PO_4, 25 mg.L^{-1} NaCl, 11.4 mg.L^{-1} H_3BO_3, alkaline EDTA solution (50 mg.L^{-1} EDTA, 31 mg.L^{-1} KOH), acidified Iron solution (5 mg.L^{-1} $FeSO_4 \cdot 7H_2O$, 1 mg.L^{-1} H_2SO_4), trace metal solution (8.8 mg.L^{-1} $ZnSO_4 \cdot 7H_2O$, 1.4 mg.L^{-1} $MnCl_2 \cdot 4H_2O$, 0.7 mg.L^{-1} MoO_3, 1.6 mg.L^{-1} $CuSO_4 \cdot 5H_2O$, 0.5 mg.L^{-1} $Co(NO_3)_2 \cdot 6H_2O$, 8.4 mg.L^{-1} $NaHCO_3$, 4.77 g.L^{-1} HEPES buffer. The inoculum was cultivated in 500 mL glass flasks, with a 200 mL working volume, continuously mixed by a shaking table operated at 150 rpm. Cultivation was performed under homogeneous and continuous 100 μmol m^{-2}. s^{-1} (cool white fluorescent lamps) light intensity and at a constant temperature of 25 °C. The HEPES buffer was applied for maintaining the pH of the cultivation medium at a value of 8 ± 0.5 during biomass growth. Biomass growth was controlled according to a previously tested standard procedure (Liu and Vyverman, 2015). More specifically, this procedure recommends re-inoculating into a new medium when the exponential phase growth condition (commonly 3 days after inoculation, when optical density (OD) is 0.6 abs) is reached.

2.2. Experimental setup

Two different mixing systems were employed for conducting the experiments in order to investigate their effect, if any, on bioflocculation: these consist in a shaking table and an air bubbling system. Cultivation on a shaking table (ST) was performed using 250 mL glass flasks, with 100 mL of working volume containing the cultivation medium and covered by a layer of cotton wool, thick enough to ensure gas exchange and to avoid loss of liquid. Different amounts of solution were used in the two systems since the same surface of liquid exposed to light was reproduced: in the bubbling system, the tubes (4 cm of length) were exposed to vertical light and for the shaking table, flasks of 100 mL created the same surface with the light coming from above. The shaking table was operated at 150 rpm. Light was continuously supplied by cool white fluorescent lamps at 100 μmol s^{-1}. m^{-2} intensity. Room temperature was maintained at 25 ± 2 °C. Cultivation of the inoculum with an air bubbling system was performed in a multi-cultivator system (MC 1000 – OD, PSI, Czech Republic) composed of eight cultivation tubes filled with 80 mL of cultivation medium and maintained under temperature-, light- and ventilation-controlled conditions. The cultivation tubes were immersed in a temperature-controlled water bath at 25 ± 0.5 °C. Each tube was illuminated with an array of LEDs that globally generated an incident irradiance of 100 μmol s^{-1}m^{-2}. The air bubbling system employed for maintaining the biomass in suspension was fed by an external air pump, supplying, for each cultivation tube, 20 ± 3 mL min^{-1} of artificially humidified air. Cultivation was carried out in batch conditions until the declining phase of growth was reached. This phase occurred for both mixing systems at day 9 of incubation. The same modified BBM was used for the cultivation medium as that of the inoculum. Prior to use, the inoculum was centrifuged for 20 min at 18,500 rpm and the resulting pellets were re-suspended in the cultivation medium. Three different stock solutions containing inocula with different initial biomass concentrations (IBC) of 10^4, 10^5, 10^6 cells. mL^{-1} were prepared. Each solution was then divided between tests using the shaking table and air bubbling as mixing systems, respectively. Tests were conducted in triplicate for both cultivation systems.

2.3. Methods

2.3.1. Biomass growth and nutrient removal

Biomass growth was monitored by optical density (OD) at 620 nm, which is the wavelength associated to the phycocyanin content. Phycocyanin is a typical pigment in cyanobacteria biomass (Stanier et al., 1979). Total suspended solids (TSS) were determined according to a standard method procedure (APHA/AWWA/WEF, 2012) in order to progressively measure, as a function of time, the dry cell weight of produced biomass. A linear correlation (Eq. (1)) was observed between the TSS content and the relative OD values:

$$\mathrm{TSS}\left(\mathrm{mg.L^{-1}}\right) = 1022.2 * \mathrm{OD620nm} + 34.466;\ R^2 = 0.9998 \quad (1)$$

Biomass growth was monitored daily by collecting the sample in suspended conditions during the experiments.

2.3.2. Evaluation of biomass settling and biomass recovery

Settling tests were performed in 100 mL glass tubes after the air bubbling and shaking table were switched off. Tests were conducted in duplicate. Tubes containing 80 mL of sample were placed in stable vertical positions into a box where static and light-controlled conditions were maintained. Both settling velocity and dynamics, were evaluated by photography (Canon EOS 7D model) at specific scheduled times. Results of settling tests covered 50 min of observation: after this time-range, no significant variations were found. The photographs were further analysed using ImageJ software (NIH, USA).

During the processing of the pictures, each pixel was converted into a numerical value proportional to the intensity of grey. This method allowed for a correlation between OD values and grey intensity at different observation times to be established (Eq. (2)):

$$\mathrm{OD620nm(abs)} = -0.0054 * \mathrm{Mean\ Grey} + 0.977;\ R^2 = 0.9267 \quad (2)$$

Eq. (2) provides an indirect estimation of the biomass concentration of the cultivation medium from photograph processing. OD values were calculated for the cultivation medium sampled at the centred half height

of the tube. For photograph processing using Image J software, a square was drawn in the centred half height of each tube and the relative pixels were converted into grey scales (commands: "transform, Image to Results"). As a consequence, each square was converted into a matrix; the average value of the matrix, termed "Mean Grey", was used in Eq. (2). This method was repeated at different cultivation times.

Biomass recovery (BR) during the settling tests was assessed on samples collected at the centred half height of each tube by comparing the OD values at 620 nm at time zero (OD 620°) with those calculated after 50 min (OD 620^{50}) (Salim et al., 2011):

$$BR(\%) = \frac{OD\ 620^{0} - OD\ 620^{50}}{OD\ 620^{0}}\% \quad (3)$$

The dynamics of biomass settling with time were assessed using image analysis during which a rectangle was drawn in the picture around the liquid working volume for each tube. For each rectangle, a grey profile was obtained, illustrating the variation of grey colour intensity along the tube. The grey profiles highlighted different trends with time, which were analysed in order to simulate biomass settling (Fig. A1 in Appendix A). Grey values were correlated to OD values using Eq. (2). Simultaneously, OD values were correlated to cell concentrations in order to obtain results in terms of particle settling as well.

Cell concentrations were evaluated, in cells. mL^{-1}, using a Malassez chamber for samples with cells in suspension. The measured concentrations were correlated to the relative OD values according to the following experimental correlation (Eq. (4)):

$$C = \left[1.0\ 10^{7} \mathrm{OD}\ 620(\mathrm{abs}) + 2.9\ 10^{5}\right](\mathrm{cells}\ /\ \mathrm{mL}) \quad (4)$$

Cell concentration profiles were used for modelling the sedimentation process. The first and last centimetres of the profiles were not taken into account for the modelling activity in order to avoid side effects due to the meniscus at the surface of the liquid as well as the tube curvature at the bottom.

2.3.3. Biomass flocculation

Biomass flocculation was studied in terms of floc sizes, shapes and microbial composition. After sedimentation, a sub-sample (1 mL) of the particulate phase was collected and analysed using a stereo zoom microscope (Leica Microsystems, M 205 FA). The relative images were captured with a dedicated camera (Leica Microsystems, camera DFC 495). Particle size analysis was conducted using ImageJ (NIH, USA). The initial dimension of the images was converted into 8 bits and thresholded. After transformation of the image, particles with an area greater than 1 mm^2 were isolated and their area calculated. Analyses were based on both maximum and average floc areas. The microbial composition of the settled biomass was assessed using an optical microscope (Olympus BX53F) and images were captured with a dedicated camera (micro Olympus, DP 80). Biomass characterisation was based on morphological features and according to literature databases.

3. Results and discussion

3.1. Inoculum characterisation

The inoculum was mainly composed of two strains of cyanobacteria, identified by their morphological features as *Pseudanabaena* sp. and *Leptolyngbya* sp. *Pseudanabaena* sp. is a filamentous cyanobacterium. Its filaments (trichomes) grow either solitary or agglomerated in very fine mucilaginous mats that can be straight, slightly wavy or arcuate. The trichomes comprise cylindrical cells, usually with slight constrictions at the distinct cross walls and are much longer than wide (0.8 vs 3 μm). *Leptolyngbya* sp. is also a filamentous cyanobacterium with filaments composed of single trichomes (chains of cells) that have straight to wavy shapes and show a lack of conspicuous motility. The trichomes are slightly constricted at the cross-walls; cells are 1.3–3.3 fold longer than wide and the end cells are rounded. They can grow solitary or coiled into clusters and fine mats (sometimes reaching macroscopic dimensions with a diameter of several centimetres), with arcuate, waved or intensely coiled aspects (Taton et al., 2012). A combination of the two filamentous cyanobacteria showed a tendency to form flocs in suspension in the liquid culture. Flocs remained suspended during the cultivation although they could easily settle when the cultivation system changed from mixed to static conditions.

3.2. Biomass growth

For both mixing systems (i.e. shaking table and air bubbling system), cyanobacteria biomass growth presented four typical phases (Richmond, 2004): lag, exponential, stationary and declining phases (Fig. 1).

The resulting trend for biomass growth was similar for both shaking table and air bubbling mixing systems and no significant difference was observed between the various IBC tested. Performing a multivariate analysis of variance (MANOVA) on data plotted in Fig. 1 with a significance level set at 0.05, neither initial biomass concentration or different cultivation system show a statistical evidence in affecting the biomass growth. The results from MANOVA reported in the following lines prove this assertion:

- ($F = 2.508$; $DF = 2, 57$; p-value<0.090) concerning the comparison among the 3 different biomass concentrations (IBC), i.e. 10^4, 10^5, 10^6 cell/mL, in shaking table (ST) system tests;
- ($F = 0.240$; $DF = 2, 54$; p-value<0.787) concerning the comparison among the 3 different biomass concentrations (IBC), i.e. 10^4, 10^5, 10^6 cell/mL, in air bubbling system in multi-cultivator (MC) tests;
- ($F = 1.633$; $DF = 1, 40$; p-value<0.209) concerning the comparison between the 2 different cultivation systems, i.e. ST and MC, at the initial biomass concentration (IBC) of 10^4 cell/mL;
- ($F = 0.027$; $DF = 1, 37$; p-value<0.869) concerning the comparison between the 2 different cultivation systems, i.e. ST and MC at the initial biomass concentration (IBC) of 10^5 cell/mL;
- ($F = 1.153$; $DF = 1, 34$; p-value<0.698) concerning the comparison between the 2 different cultivation systems, i.e. ST and MC at the initial biomass concentration (IBC) of 10^6 cell/mL.

The mixing system therefore did not affect the biomass growth trend. A lower IBC resulted in a longer initial lag-phase, whereas the higher biomass concentration promoted a faster biomass adaptation and growth. Accordingly, the declining phase occurred later for the lowest IBC. This phase occurred during each test when the OD in the cultivation medium was close to 1.00 abs. This result is likely due to light limitation when the density of cyanobacteria biomass is high, or alternatively, due to nutrient depletion in the cultivation medium (Xin et al., 2010; Sutherland et al., 2015). It could also result from the combination of both phenomena (i.e. light limitation and nutrient depletion).

3.3. Biomass settling model and dynamics

The settling tests resulted in very different profiles compared to the customary zone-settling behaviour reported in the literature for activated sludge (Vanderhasselt and Vanrolleghem, 2000; Takács et al., 1991; Li and Stenstrom, 2014; Kynch, 1952), showing no apparent interface between the clarified supernatant and settling particles. For the filamentous cyanobacteria consortium, sedimentation differs from activated sludge principally because cyanobacteria form flocs of larger sizes compared to heterotrophic activated sludge bacteria (Inoue et al., 2016). Furthermore, the two most abundant cyanobacteria species in the consortium demonstrate different morphological characteristics, which can affect the formation of flocs and their settlement.

Particle sedimentation is assumed to be governed by steady gravitational drift and diffusion, and was modelled according to the Mason-Weaver equation (Eq. (5)) based on two populations of particles:

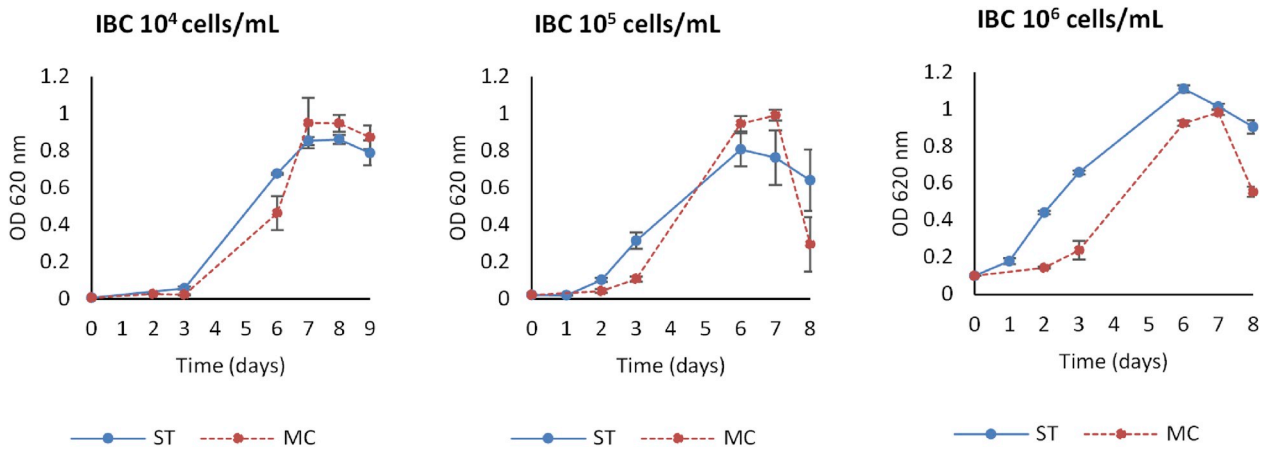

Fig. 1. Biomass concentration as a function of time for different initial biomass concentrations (IBC) and for the two cultivating systems: shaking table (ST) and air bubbling in multi-cultivator (MC).

$$\frac{dC}{dt} = f_1\left(D_1\frac{d^2C}{dz^2} + v_1\frac{dC}{dz}\right) + f_2\left(D_2\frac{d^2C}{dz^2} + v_2\frac{dC}{dz}\right) \quad (5)$$

where f_i is the C_i/C ratio of biomass i compared to the total biomass. D_i and v_i are the diffusion coefficient (cm^2/s) and the settling velocity of biomass i (cm/s) respectively.

In steady state conditions, the concentration profile as a function of height z (cm) is thus represented by (Eq. (6)):

$$C(z) = C_0\left(f_1 e^{-\frac{z}{D_1/v_1}} + f_2 e^{-\frac{z}{D_2/v_2}}\right) \quad (6)$$

C_0 (cells/mL) was estimated from homogeneous concentration profiles at time $t = 0$. Parameters f_i and D_i/v_i were evaluated on concentration profiles after 50 min of settling. Population 1 corresponds to "suspended cells" that settle only slightly, while population 2 correspond to "settling cells" that settle efficiently. On one hand, parameters for population 1 were thus estimated by a linear regression method on ln (C) of the upper part ($z > 3$ cm, green line in Fig. 2) of the profiles, where $C_2 \approx 0$. On the other hand, parameters for population 2 were estimated on the residues by a linear regression method on ln($C–C_1$) of the lower part of the curve ($z < 3$ cm, purple line in Fig. 2).

For experiments with highest settling fractions ($f_2 > 0.2$), sedimentation profiles after 5 min were modelled with COMSOL Multiphysics® using parameters C_0, f_1, f_2 and ratio D_1/v_1 and D_2/v_2 estimated with parametric sweeps over settling velocities v_1 and v_2. Parameters tested were 10^{-7}, 10^{-6}, 10^{-5}, 10^{-4} and 10^{-3} m/s for v_1 and from $0.1 \cdot 10^{-4}$ to $5 \cdot 10^{-4}$ m/s every $0.1 \cdot 10^{-4}$ m/s for v_2. Calculations were carried out on a 1D grid composed of 0.01 cm elements on the whole height of the liquid column measured in the experiment (H = 13.6 ± 0.9 cm), assuming the flux boundary at the upper and lower bounds of the grid are null. The best fit of the predicted sedimentation profile compared to the experimental sedimentation profile at 5 min, was selected by using the minimum residual sum of squares (RSS) criterion (Eq. (7)):

$$RSS = \sum\left(C_{measured} - C_{predicted}\right)^2 \quad (7)$$

Thanks to this procedure, values could be assigned to v_1, D_1, v_2 and D_2 parameters for each investigated case. It also allowed for a complete simulation of the settling dynamics as shown in Fig. 3.

Measured and modelled concentration profiles at time t = 0 min and t = 50 min (end of settling) are illustrated in Figs A2 and A3 in Appendix A for the shaking table and air bubbling mixing system, respectively.

The model fitting procedure provided the D/v ratio and the relative proportions for both populations (Table 1). Taking into account all experiments, the D/v ratio was 32 ± 14 cm for population 1, and 0.58 ± 0.14 cm for population 2. As expected, these values indicate a poor settling efficiency for population 1 with $D_1/v_1 >$ H (tube height) and a settling phenomenon mainly governed by diffusion. Indeed, the settling profile was only slightly different from the homogenous distribution (see Fig. 2) found at time t = 0. On the contrary, population 2 settled efficiently with $D_2/v_2 \ll$ H and a settling phenomenon mainly governed by the gravitational drift (Fig. 2).

For both cultivation systems, the percentage of population 2 (f2, i.e. particles that settle efficiently due to dominance of gravitational drift) increases during the cultivation time for the IBC of 10^4 and 10^5 cells/mL, while for the IBC of 10^6 cells/mL, it increases until day 7, after which it decreases again (see Fig. A4 of Appendix A). This result, together with the growth trend (shown in Fig. 1), is crucial for understanding the settling dynamics of biomass: settling was fast during the exponential growth phase, and began to slow down during the declining phase. Interestingly, the shaking table (ST) and air bubbling in multi-cultivator (MC) systems showed different characteristics for population 2, whose percentage is higher for the MC system. The values of the D_2/v_2 ratios are 0.70 ± 0.06 cm for ST and 0.45 ± 0.06 cm for MC (Table 1); consequently, air bubbles favour the formation of particles that can settle more efficiently (low D_2/v_2). Finally, the highest percentage of particles that settle efficiently (57%) was reached for the highest IBC, for the Multicultivator system and at the end of the exponential growth phase (day 7): this combination represents the most favourable

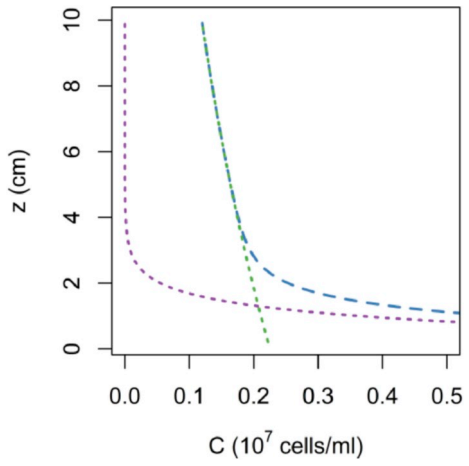

Fig. 2. Cell concentration profiles predicted by the model for population 1 in green, population 2 in purple and for the global population in blue. (For interpretation of the references to colour in this figure legend, the reader is referred to the Web version of this article.)

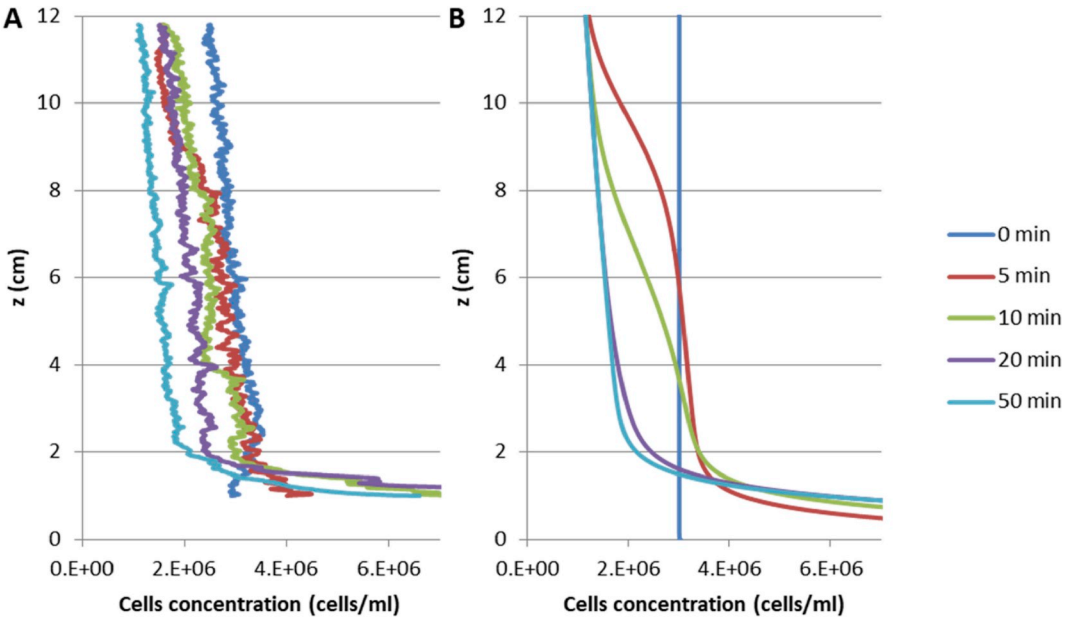

Fig. 3. Measured (A) and modelled (B) sedimentation profiles at different sedimentation times for MC IBC 10^5 cells/ml day 8 experiment.

Table 1
D/v ratios and relative proportions of populations 1 and 2 estimated from the modelling of experiments with shaking table (ST) and air bubbling in multi-cultivator (MC) systems for various Initial Biomass Concentrations (IBC).

ST, IBC 10^4 (cells/l)					ST, IBC 10^5 (cells/l)					ST, IBC 10^6 (cells/l)				
	day 6	**day 7**	**day 8**	**day 9**		**day 3**	**day 6**	**day 7**	**day 8**		**day 3**	**day 6**	**day 7**	**day 8**
D1/v1 (cm)	24	24	22	32	**D1/v1 (cm)**	31	54	28	21	**D1/v1 (cm)**	35	27	31	30
f1	98%	91%	83%	77%	**f1**	99%	91%	73%	62%	**f1**	92%	80%	75%	78%
D2/v2 (cm)	0.22	0.78	0.95	0.76	**D2/v2 (cm)**	0.69	0.91	0.64	0.71	**D2/v2 (cm)**	2.58	0.74	0.62	0.73
f2	2%	9%	17%	23%	**f2**	1%	9%	27%	38%	**f2**	8%	20%	25%	22%
MC, IBC 10^4 (cells/l)					**MC, IBC 10^5 (cells/l)**					**MC, IBC 10^6 (cells/l)**				
	day 6	**day 7**	**day 8**	**day 9**		**day 3**	**day 6**	**day 7**	**day 8**		**day 3**	**day 6**	**day 7**	**day 8**
D1/v1 (cm)	58	77	48	28	**D1/v1 (cm)**	20	32	26	21	**D1/v1 (cm)**	29	26	19	16
f1	100%	99%	87%	68%	**f1**	99%	95%	72%	51%	**f1**	96%	72%	43%	60%
D2/v2 (cm)	2.95	0.93	0.78	0.51	**D2/v2 (cm)**	0.18	0.73	0.48	0.40	**D2/v2 (cm)**	0.55	0.44	0.37	0.53
f2	0%	1%	13%	32%	**f2**	1%	5%	28%	49%	**f2**	4%	28%	57%	40%

condition for settling.

According to the modelled steady-state profile, 95% of cells from population 2 are estimated to be found at a distance $3D_2/v_2$ from the bottom of the tube, i.e. an average 2.1 cm for the shaking table system and an average 1.3 cm for the air bubbling system. The amount of biomass associated to population 2 can thus be considered recoverable and efficiently harvested for further processing.

In order to provide more details on the sedimentation dynamics, settling velocities for population 2 were evaluated through simulation of sedimentation for tests where the recoverable amount of biomass was above 20% of the total biomass (Table 2). Such settling velocities are in agreement with those estimated by Francois *at al.* for activated sludge settling (François et al., 2016).

The simulated settling behaviour is also reported in an animated image in the online supplementary materials (settling simulation video. gif). The measured settling velocities ranged between $0.5 \cdot 10^{-4}$ and $3.7 \cdot 10^{-4}$ m/s (Table 2), with the highest velocity obtained for IBC 10^6 cells/ml at day 7 in the air bubbling mixing system. In the shaking table mixing system, slower kinetics were measured with a maximal velocity of $2.4 \cdot 10^{-4}$ m/s at day 8 for tests conducted with IBC 10^5 cells/ml, when the highest percentage of faster settling particles (f2) was also reached (see Table 1).

Supplementary video related to this article can be found at https://doi.org/10.1016/j.jenvman.2019.109957

Table 2
-Settling velocities for population 2 in experiments with f2 > 20% in shaking table (ST) and air bubbling in multi-cultivator (MC) systems for various Initial Biomass Concentrations (IBC).

	v_2 (m/s)					
	ST			MC		
Day	IBC 10^4 cells/mL	IBC 10^5 cells/mL	IBC 10^6 cells/mL	IBC 10^4 cells/mL	IBC 10^5 cells/mL	IBC 10^6 cells/mL
6			5.0E-05			5.0E-05
7		8.0E-05	2.4E-04		1.1E-04	3.7E-04
8		2.1E-04	1.6E-04		1.1E-04	1.5E-04
9	7.0E-05			6.0E-05		

3.4. Biomass recovery

The amount of recoverable biomass was evaluated with OD measurements after 50 min of settling according to Eq. (3). The relative values are shown in Fig. 4.

The maximum amount of recoverable biomass resulted in 70% of the total biomass. The recoverable amount of biomass increases with time for each test except for tests conducted with the highest IBC (10^6 cells/ml) when the recoverable amount decreased during the last days of observation. Moreover, globally, at the end of cultivations, the air

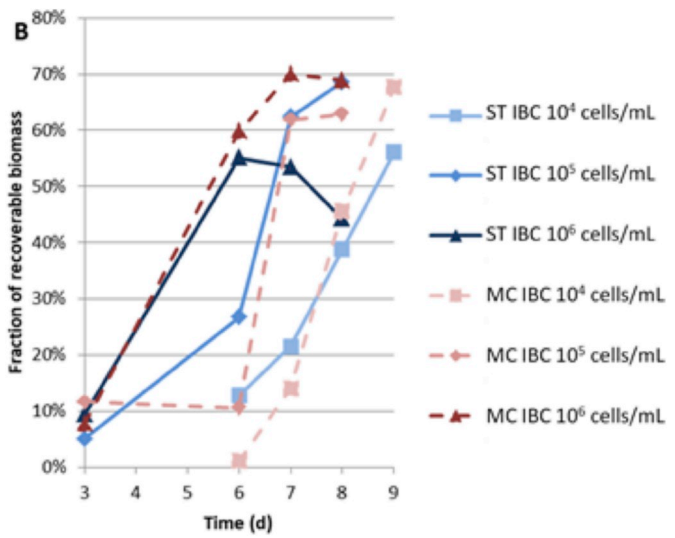

Fig. 4. Fraction of recoverable biomass calculated from OD measurements as function of cultivation time for shaking table (ST) system (blue plain lines) and air bubbling in multi-cultivator (MC) system (red dashed lines) with various Initial Biomass Concentrations (IBC). (For interpretation of the references to colour in this figure legend, the reader is referred to the Web version of this article.)

bubbling mixing system resulted in better biomass recovery than the shaking table system. Finally, the highest recovery was obtained for the air bubbling mixing system with the highest IBC (10^6 cells/ml) at day 7. Interestingly, this day coincides with the end of the stationary phase of this test (see Fig. 1).

The physiological growth state proved to be the main factor influencing biomass recovery: low sedimentation performances were observed during the exponential growth phase, while the stationary state growth phase promoted natural flocculation (bioflocculation) that enhanced biomass sedimentation.

The formation of flocs with time was monitored by stereomicroscope analysis (Fig. 5). For the shaking table system, when the IBC was set at 10^6 cells/mL, floc formation occurred very rapidly, i.e. after one day of cultivation. From day 1–3, floc sizes increased for the shaking table mixing system although their shapes became progressively looser. For the air bubbling mixing system with the same value of IBC (i.e. 10^6 cells/mL), flocs only became visible after 3 days of cultivation. As a result, such flocs were smaller but denser than those produced with the shaking table mixing system at the same cultivation time. This difference could be explained by the different shear stress conditions induced on the biomass by the two mixing systems. More specifically, the air bubbles interacted directly with the biomass flocs and inhibited their formation during the first 3 days. The same shear stress limited the size of the flocs, and thus promoted their dense and rounded shapes. On the contrary, the oscillatory movements favoured interactions between the particles forming the suspended biomass. As a consequence, floc formation had already occurred in the shaking table mixing system after the first day of cultivation thanks to the agglomeration of the inoculated biomass.

Floc size analysis is reported in Table 3. During the first 3 days, the highest average floc sizes were observed for the highest IBC. This result implies that the new biomass tended to floc in aggregates since biomass growth favoured increasing floc sizes. At day 7, the average floc sizes reached the same value of 8.0 ± 0.3 mm^2 for all IBC tested in the 10^4-10^6 cells/mL range. This size value was reached when the same biomass concentration (OD of 1 absorbance unit at 620 nm) was reached in all shaking table cultures (Fig. 1). As result, the IBC does not affect floc sizes since it rather seems to depend on the biomass concentration in the culture. In the air bubbling mixing system, flocs were generally smaller in size (i.e. 3.8 ± 0.1 mm^2 compared to14.0 ± 4.3 mm^2 obtained with the shaking table system), but they presented a higher level of homogeneity. For an IBC lower than 10^6 cells/mL, floc sizes remained small,

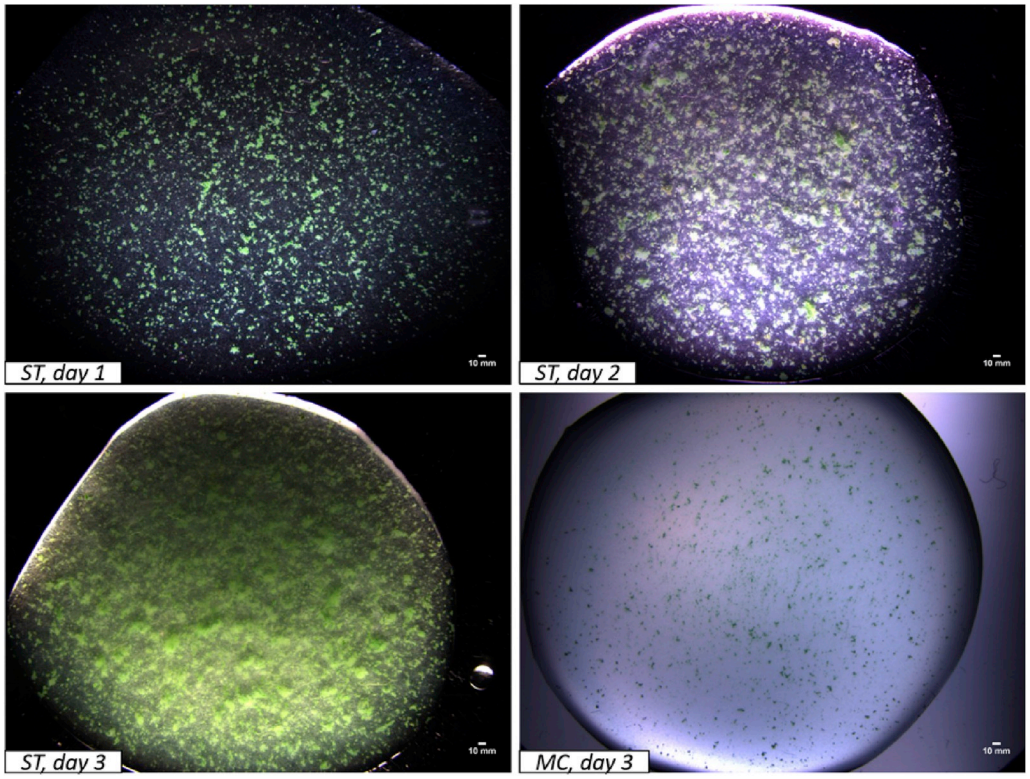

Fig. 5. Stereomicroscope pictures (e. t. ¼ sec) in time for the shaking table (ST) and multicultivator (MC) samples with the initial biomass concentration of 10^6 cells/mL.

Table 3
Floc size analysis for shaking table (ST) and air bubbling in multi-cultivator (MC) systems as well as for the different IBC.

Flocs area (mm^2)		Time (d)			
		1	2	3	7
ST, ibc 10^4 cells/mL	*Max*			52.4 ± 2.8	166.3 ± 1.9
	Average			5.9 ± 1.1	7.7 ± 0.7
ST, ibc 10^5 cells/mL	*Max*		24.6 ± 1.9	88.3 ± 3.8	178.4 ± 1.9
	Average		5.0 ± 0.7	8.8 ± 2.0	8.5 ± 0.8
ST, ibc 10^6 cells/mL	*Max*	93.2 ± 1.9	156.1 ± 1.8	170.4 ± 1.9	72.2 ± 1.9
	Average	10.6 ± 4.2	14.7 ± 0.6	14.0 ± 4.3	7.9 ± 0.8
MC, ibc 10^6 cells/mL	*Max*			28.7 ± 4.8	13.9 ± 1.8
	Average			3.8 ± 0.1	2.1 ± 0.2

so the results were not reported in Table 3. Finally, for both cultivation systems, floc sizes generally decreased after the exponential growth phase.

Biomass composition analysis also contributed to explain the different floc shapes and sizes observed in the two different mixing systems. At time t = 0, the biomass composition, corresponding to the inoculum, was the same for both systems. However, during cultivation, the biomass composition of the settled flocs differed in the two systems. Pictures captured from microscope analysis are reported in Fig. 6 for the settled biomass collected at day 6 for the shaking table (top) and air bubbling (bottom) mixing systems. For the shaking table, the flocs contained two species of cyanobacteria, the same that formed the inoculum. More specifically, the structure of the flocs comprised an internal and dense nucleus of *Pseudanabaena* filaments and external hairs composed of *Leptolyngbya* filaments. For the air bubbling system, *Pseudanabaena* sp. was the predominant species and proved to be responsible for forming small but dense and well-shaped floc structures. Consequently, the biomass mixing system appears to affect biomass speciation. Indeed, the higher shear stress generated by the air bubbling system limits the growth of *Leptolyngbya* filaments. Their typical morphology is longer and thinner than that of *Pseudananbaena* sp., so they are more fragile. On the contrary, *Pseudanabaena* filaments are shorter and wider and they are capable of sticking together in dense and well-structured flocs. Therefore, in terms of biomass sedimentation, flocs formed with the air bubbling mixing system were heavy and tended to settle more easily and faster, while flocs formed with the shaking table mixing system settled more slowly because of their low density and hairy structures.

The biomass growth phase also influenced the features of the flocs, as illustrated by stereomicroscope pictures (Fig. A5 in Appendix A) captured at different times for the shaking table system: flocs began to form after one day thanks to filament gliding and to the biomass mixing system. Varying shades of green indicated a higher density of biomass at the centre of the floc than at its boundary. Floc formation therefore originates from bridging between both free filaments and free flocs. At day 7, during the declining phase, the colour of the biomass turned from green to yellow and subsequent breaking of flocs occurred. The death of the cyanobacteria caused the filaments to disaggregate from the floc, resulting in a low density and dispersed configuration.

4. Conclusions

The present work demonstrates how bioflocculation of cyanobacteria can be obtained from different mixing systems, such as air bubble and shaking movements; moreover, the bioflocculation process induces a natural settling of biomass which allows for the recovery of up to 70% of the total cultivated biomass.

Both initial biomass concentrations (IBC) and mixing systems affected the biomass settling dynamics; indeed the air bubbling mixing system associated to the highest IBC promoted the most efficient

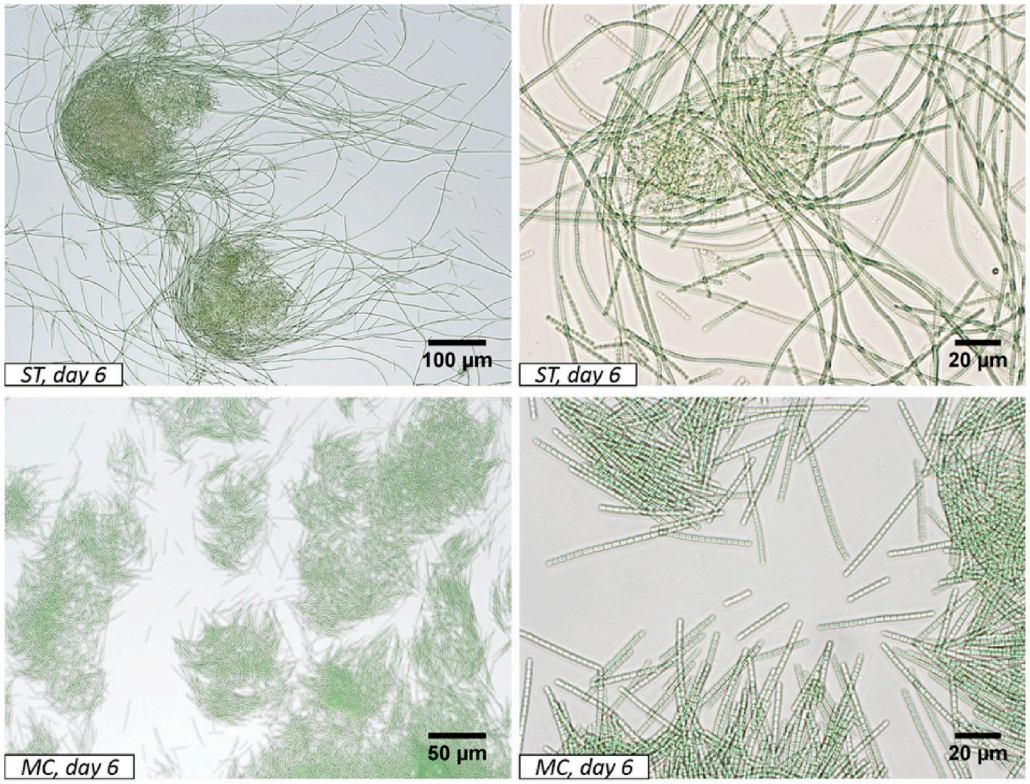

Fig. 6. Optical microscope pictures of settled biomass in the shaking table (ST) and air bubbling in multi-cultivator (MC) systems with the initial biomass concentration of 10^4 cells/mL.

biomass settling rate. Biomass settling was also found to be related to the biomass growth phase, with faster settling rates during the exponential growth phase and slower settling rates when the biomass began to decline.

This work also demonstrates how the biomass mixing system affects biomass speciation and, as a consequence, the floc structures. The natural settling behaviour of the biomass can be modelled based on the overlapping sedimentation of two populations of particles: particles that do not settle due to dominance of diffusion and particles that settle efficiently due to gravitational drift. The microscope analysis of flocs confirmed this hypothesis, since the densest flocs were associated to the faster settling biomass (gravitational settling mode), while the largest but less dense flocs comprised the slowest settling biomass (diffusivity settling mode). By modelling biomass settling merely from the analysis of settling images, calculations of settling dynamics (settling velocity, settling rate) can be made, allowing for the prediction of the settling behaviour and even the composition of the biomass.

These noteworthy results, achieved on filamentous cyanobacteria bioflocculation, could promote further investigations on this inexpensive method of natural settling, with the objective of improving their recovery. Additionally, the bioflocculation performances observed for these species could enhance the recovery of other organisms, such as microalgae, that could be trapped within cyanobacterial flocs. Finally, this process would become even more economically sustainable if wastewater were used as growth medium for the cyanobacteria species.

E-supplementary data of this work can be found in online version of the paper.

Declaration of competing interest

The authors report no declarations of interest.

Acknowledgements

This study was supported by PHYCOVER project, which was funded by the French National Agency for Research (ANR-14-CE04-0011). The authors are grateful to the French National Institute for Agricultural Research (INRA – LBE, Laboratoire de Biotechnologie de l'Environment), University of studies of Molise - Bioscience and Territory department, University of Naples Federico II – Civil, Architectural and Environmental Engineering department for supporting this work; they thank all the other members of LBE for their advice.

Appendix A. Supplementary data

Supplementary data to this article can be found online at https://doi.org/10.1016/j.jenvman.2019.109957.

References

Alam, M.A., Vandamme, D., Chun, W., Zhao, X., Foubert, I., Wang, Z., Muylaert, K., Yuan, Z., 2016. Bioflocculation as an innovative harvesting strategy for microalgae. Rev. Environ. Sci. Biotechnol. 1–11. https://doi.org/10.1007/s11157-016-9408-8.

APHA/AWWA/WEF, 2012. Standard methods for the examination of water and wastewater. Stand. Methods. 541. ISBN 9780875532356.

Barros, A.I., Gonçalves, A.L., Simões, M., Pires, J.C.M., 2015. Harvesting techniques applied to microalgae: a review. Renew. Sustain. Energy Rev. 41, 1489–1500. https://doi.org/10.1016/j.rser.2014.09.037.

Castenholz, R.W., 1967. Aggregation in a thermophilic oscillatoria [23]. Nature 215, 1285–1286. https://doi.org/10.1038/2151285a0.

Christenson, L., Sims, R., 2011. Production and harvesting of microalgae for wastewater treatment, biofuels, and bioproducts. Biotechnol. Adv. 29, 686–702. https://doi.org/10.1016/j.biotechadv.2011.05.015.

François, P., Locatelli, F., Laurent, J., Bekkour, K., 2016. Experimental study of activated sludge batch settling velocity profile. Flow Meas. Instrum. 48, 112–117. https://doi.org/10.1016/j.flowmeasinst.2015.08.009.

Gouveia, L., Graça, S., Sousa, C., Ambrosano, L., Ribeiro, B., Botrel, E.P., Neto, P.C., Ferreira, A.F., Silva, C.M., 2016. Microalgae biomass production using wastewater: treatment and costs. Scale-up considerations. Algal Res 16, 167–176. https://doi.org/10.1016/j.algal.2016.03.010.

Inoue, D., Suzuki, Y., Uchida, T., Morohoshi, J., Sei, K., 2016. Polyhydroxyalkanoate production potential of heterotrophic bacteria in activated sludge. J. Biosci. Bioeng. 121, 47–51. https://doi.org/10.1016/j.jbiosc.2015.04.022.

Koblížek, M., Komenda, J., 2000. Cell aggregation of the cyanobacterium Synechococcus elongatus: role of the electron transport chain. J. …. 668, 662–668. https://doi.org/10.1046/j.1529-8817.2000.99030.x.

Kynch, G.J., 1952. A theory of sedimentation. Trans. Faraday Soc. 48, 166. https://doi.org/10.1039/tf9524800166.

Lardon, L., Hélias, A., Sialve, B., Steyer, J.-P., Bernard, O., 2009. Life-cycle assessment of biodiesel production from microalgae. Environ. Sci. Technol. 43, 6475–6481. https://doi.org/10.1021/es900705j.

Li, B., Stenstrom, M.K., 2014. Research advances and challenges in one-dimensional modeling of secondary settling Tanks - a critical review. Water Res. 65, 40–63. https://doi.org/10.1016/j.watres.2014.07.007.

Liu, J., Vyverman, W., 2015. Differences in nutrient uptake capacity of the benthic filamentous algae Cladophora sp., Klebsormidium sp. and Pseudanabaena sp. under varying N/P conditions. Bioresour. Technol. 179, 234–242. https://doi.org/10.1016/j.biortech.2014.12.028.

Ndikubwimana, T., Zeng, X., He, N., Xiao, Z., Xie, Y., Chang, J.S., Lin, L., Lu, Y., 2015. Microalgae biomass harvesting by bioflocculation-interpretation by classical DLVO theory. Biochem. Eng. J. 101, 160–167. https://doi.org/10.1016/j.bej.2015.05.010.

Park, J.B.K., Craggs, R.J., Shilton, A.N., 2015. Algal recycling enhances algal productivity and settleability in Pediastrum boryanum pure cultures. Water Res. 87, 97–104. https://doi.org/10.1016/j.watres.2015.09.013.

Pradhan, N., Dipasquale, L., Ippolito, G., Panico, A., Lens, P.N.L., Esposito, G., Fontana, A., 2017. Hydrogen and lactic acid synthesis by the wild-type and a laboratory strain of the hyperthermophilic bacterium Thermotoga neapolitana DSMZ 4359 T under capnophilic lactic fermentat ScienceDirect Hydrogen and lactic acid synthesis by the wild-type and a laboratory strain of the hyperthermophilic bacterium Thermotoga neapolitana DSMZ 4359 T under capnophilic lactic fermentation conditions. Int. J. Hydrogen Energy. https://doi.org/10.1016/j.ijhydene.2017.05.052.

Richmond, A., 2004. Handbook of microalgal culture: biotechnology and applied phycology/edited by Amos Richmond. Orton.Catie.Ac.Cr 472. https://doi.org/10.1002/9780470995280.

Salim, S., Bosma, R., Vermuë, M.H., Wijffels, R.H., 2011. Harvesting of microalgae by bio-flocculation. J. Appl. Phycol. 23, 849–855. https://doi.org/10.1007/s10811-010-9591-x.

Shepard, R.N., Sumner, D.Y., 2010. Undirected motility of filamentous cyanobacteria produces reticulate mats. Geobiology 8, 179–190. https://doi.org/10.1111/j.1472-4669.2010.00235.x.

Singh, V., Chaudhary, D.K., Mani, I., Dhar, P.K., 2016. Recent advances and challenges of the use of cyanobacteria towards the production of biofuels. Renew. Sustain. Energy Rev. 60, 1–10. https://doi.org/10.1016/j.rser.2016.01.099.

Stanier, R.Y., Deruelles, J., Rippka, R., Herdman, M., Waterbury, J.B., 1979. Generic assignments, strain histories and properties of pure cultures of cyanobacteria. Microbiology 111, 1–61. https://doi.org/10.1099/00221287-111-1-1.

Su, Y., Mennerich, A., Urban, B., 2011. Municipal wastewater treatment and biomass accumulation with a wastewater-born and settleable algal-bacterial culture. Water Res. 45, 3351–3358. https://doi.org/10.1016/j.watres.2011.03.046.

Sutherland, D.L., Howard-Williams, C., Turnbull, M.H., Broady, P.A., Craggs, R.J., 2015. Enhancing microalgal photosynthesis and productivity in wastewater treatment high rate algal ponds for biofuel production. Bioresour. Technol. 184, 222–229. https://doi.org/10.1016/j.biortech.2014.10.074.

Takács, I., Patry, G.G., Nolasco, D., 1991. A dynamic model of the clarification-thickening process. Water Res. 25, 1263–1271. https://doi.org/10.1016/0043-1354(91)90066-Y.

Taton, A., Lis, E., Adin, D.M., Dong, G., Cookson, S., Kay, S.A., Golden, S.S., Golden, J.W., 2012. Gene transfer in Leptolyngbya sp. strain BL0902, a cyanobacterium suitable for production of biomass and bioproducts. PLoS One 7. https://doi.org/10.1371/journal.pone.0030901.

Vanderhasselt, A., Vanrolleghem, P.A., 2000. Estimation of sludge sedimentation parameters from single batch settling curves. Water Res. 34, 395–406. https://doi.org/10.1016/S0043-1354(99)00158-X.

Xin, L., Hong-ying, H., Ke, G., Ying-xue, S., 2010. Effects of different nitrogen and phosphorus concentrations on the growth, nutrient uptake, and lipid accumulation of a freshwater microalga Scenedesmus sp. Bioresour. Technol. 101, 5494–5500. https://doi.org/10.1016/j.biortech.2010.02.016.